ISSN (Online) 2456-1290

International Journal of Engineering Research in Mechanical and Civil Engineering (IJERMCE)
Vol 2, Issue 3, March 2017

Heat and Mass Transfer of TIO2-Water Nanofluid in a cylindrical annulus with non-Darcy Parameter

[1] Y. Devasena , [2] A. Haritha
Academic Consultant, School of Engineering & Technology, SPMVV, Tirupati.
[1] yellamraju.devasena@gmail.com, [2] arigalaharitha@gmail.com

***Abstract*: -- In this paper we studied Non-Darcy convective heat and mass transfer of Tio2-water nanofluids in an annular region between two concentric cylinders whose walls are maintained at constant temperature and concentration. The non-linear governing equations have been solved using Galerkine finite element analysis with quadratic approximation polynomials. The velocity, temperature and concentration are analyzed for different values of G, D-1, *α*, Sc, and . The rate of heat transfer and Skin friction at the boundaries have evaluated for different variations.**

***Key Words*: Cylindrical Annulus, Finite element technique, Non-Darcy flow, Nanofluid.**

I. INTRODUCTION

Nowadays, heat transfer attracts many researchers' as the low thermal conductivity of conventional heat transfer, fluids such as water, is assumed to be an important limitation in increasing the heat transfer performance. Maxwell's study [1] showed the possibility of enhancing the thermal conductivity of fluid-solid particles. During the past decade a new kind of solid or liquid mixture known as nanofluid in nanometer dimensions was improved. Choi [2] was the first person who proposed this nanofluids. The commonly used nanoparticles in nanofluids are oxides, carbides, metals and the base liquids like water, ethylene glycol etc. They will show high thermal conductivity and convective heat transfer coefficient when compared to the base fluid. Nanofluids have many applications in heat transfer such as solar collectors, heat exchangers, radiators etc. Wen and Ding [3] analzed the natural convection of TiO2-water in a vessel composed of two discs. Mokhtari Moghari et al,. [4] investigated the two phase mixed convection Al2O3-water nanofluid flow in an annulus. Abu-Nada [5] illustrated the effect of variable viscosity and thermal conductivity of Al2O3-water nanofluid on heat transfer enhancement in natural convection. Recently S. Srinivas et al., [6] has investigated hydromagnetic
flow of a nanofluid in porous channel with expanding or contracting walls. Nagasasikala et al., [7] analyzed the convective flow of Cuo-water and Ag-water nananofluids in a circular annulus with constant heat flux. Reddy et al [8] have investigated the non-darcy convective flow of a nanofluids in a vertical channel. Sudarsana reddy et al[9] have discussed the MHD convective heat transfer flow of Al2o3-water and Tio2-water nanofluids past a stretching sheet in porous medium with heat generation/absorption. Srinivas et al[10] have investigated particle spacing and chemical reaction effects on convective heat transfer through a nanofluids in cylindrical annulus. Sheikhzadeh et al[11] illustrated the laminar natural convection of Cu-water nanofluids in concentric annuli with radial fins attached to the inner cylinder.

In this paper we investigate non-Darcy convective heat and mass transfer flow of Tio2-water nanofluid in a cylindrical annulus with non-Darcy parameter, heat sources and chemical reaction. By employing Galerkin finite element analysis with quadratic appropriate functions the governing equations have been solved. The velocity, temperature and concentrations were investigated for different parameters like Grashof number G, Inverse Darcy parameter D-1 , Forchemmier number F, Heat source parameter $\propto$, Chemical reaction parameter γ, Schimdt number Sc, Prandatl number Pr, and nanoparticle volume fraction $\emptyset$.

II. FORMULATION OF THE PROBLEM

We consider the free and forced convection flow in a circular annulus through a porous medium whose walls are maintained at a constant heat flux and uniform concentration. Both the fluid and porous region have constant physical properties and the mixed convection flow taking place with uniform axial pressure gradient under thermal and molecular buoyancies. The Boussinesq approximation is employed so that the density variation is restricted to the thermal and molecular buoyancy forces. The Brinkman-Forchheimer extended Darcy model which involves the inertia and boundary effects has been used for the momentum equation in the porous region. The momentum, energy and diffusion equations are non linear coupled equations and the flow is assumed to be unidirectional along the axial direction of the cylindrical annulus. With the above assumptions the governing equations are

ISSN (Online) 2456-1290

International Journal of Engineering Research in Mechanical and Civil Engineering (IJERMCE)
Vol 2, Issue 3, March 2017

$$-\frac{\partial p}{\partial z}+\frac{\mu_{nf}}{\rho_{nf}\delta}\left(\frac{\partial^2 u}{\partial r^2}+\frac{1}{r}\frac{\partial u}{\partial r}\right)-\left(\frac{\mu_{nf}}{\rho_{nf}k}\right)u-\frac{\delta F}{\rho_{nf}\sqrt{k}}u^2+(\rho\beta)_{nf}(T-T_i)=0 \quad (1)$$

$$(\rho C_p)_{nf}\,u\frac{\partial T}{\partial z}=k_{nf}\left(\frac{\partial^2 T}{\partial r^2}+\frac{1}{r}\frac{\partial T}{\partial r}\right)+Q_H(T-T_0) \quad (2)$$

$$u\frac{\partial C}{\partial z}=D_B\left(\frac{\partial^2 C}{\partial r^2}+\frac{1}{r}\frac{\partial C}{\partial r}\right)-k_c^{'}C \quad (3)$$

where u is the axial velocity in the porous region, T , C are the temperature and concentration of the fluid, k is the permeability of porous medium, k_f is the thermal diffusivity, F is a function that depends on Reynolds number, the microstructure of the porous medium and D_B is the molecular diffusivity, β is the coefficient of the thermal expansion, Q_H is the heat source coefficient, Cp is the specific heat, ρ is density and g is gravity. The relevant boundary conditions are

$u=0$, T= T_w, C= C_w at r = a & a+s (4)

We assume that the temperature and concentration of the both walls is $T_w=T_0+Az$, $C_w=C_0+Bz$ where A and B are the vertical temperature and concentration gradients which are positive for buoyancy aided flow and negative for buoyancy opposed flow respectively, T_0 and C_0 are the upstream reference wall temperature and concentration respectively. The temperature and concentration inside the fluid can be written as

$$T=T^{\bullet}(r)+Az \quad , \quad C=C^{\bullet}(r)+Bz \quad (5)$$

The effective density of the nanofluid is given by

$$\rho_{nf}=(1-\varphi)\rho_f+\varphi\rho_s \quad (6)$$

Where ϕ is the solid volume fraction of nanoparticles
Thermal diffusivity of the nanofluid is

$$\alpha_{nf}=\frac{k_{nf}}{(\rho C_p)_{nf}} \quad (7)$$

Where the heat capacitance C_p of the nanofluid is obtained as

$$(\rho C_p)_{nf}=(1-\varphi)(\rho C_p)_f+\varphi(\rho C_p)_s \quad (8)$$

And the thermal conductivity of the nanofluid k_{nf} for spherical nanoparticles can be written as

$$\frac{k_{nf}}{k_f}=\frac{(k_s+2k_f)-2\phi(k_f-k_s)}{(k_s+2k_f)+\phi(k_f-k_s)} \quad (9)$$

The thermal expansion coefficient of nanofluid can determine by

$$(\rho\beta)_{nf}=(1-\varphi)(\rho\beta)_f+\varphi(\rho\beta)_s \quad (10)$$

Also the effective dynamic viscosity of the nanofluid given by

$$\mu_{nf}=\frac{\mu_f}{(1-\varphi)^{2.5}},$$

$$\sigma_{nf}=\sigma_f\left(1+\frac{3(\sigma-1)\phi}{\sigma+2-(\sigma-1)\phi}\right),\sigma=\frac{\sigma_s}{\sigma_f}$$

Where the subscripts *nf*, f and s represent the thermo physical properties of the nanofluid, base fluid and the nano solid particles respectively and ϕ is the solid volume fraction of the nanoparticles. The thermo physical properties of the nanofluid are given in Table - 1.We now define the following non-dimensional variables

$$z^*=\frac{z}{a}, \quad r^*=\frac{r}{a}, u^*=\left(\frac{a}{\nu}\right)u, p^*=\frac{pa\delta}{\rho\nu^2},$$

$$\theta^*(r^{\bullet})=\frac{T^{\bullet}-T_0}{P_1Aa} \quad , \quad C^*(r^{\bullet})=\frac{C^{\bullet}-C_0}{P_1Ba} \quad , \quad s^*=\frac{s}{a}$$

$$P_1=\frac{dp}{dx} \quad (11)$$

Introducing these non-dimensional variables, the governing equations in the non-dimensional form are

$$\left(\frac{\partial^2 u}{\partial r^2}+\frac{1}{r}\frac{\partial u}{\partial r}\right)=1+\delta(D^{-1})u+\delta^2(D^{-1})^{1/2}\Delta u^2-\delta G(\theta+NC) \quad (12)$$

$$\left(\frac{\partial^2\theta}{\partial r^2}+\frac{1}{r}\frac{\partial\theta}{\partial r}\right)=u-\frac{\alpha}{\Pr}\theta \quad (13)$$

$$\left(\frac{\partial^2 C}{\partial r^2}+\frac{1}{r}\frac{\partial C}{\partial r}\right)-\gamma C=Sc\,u \quad (14)$$

where $\Delta=FD^{-1}$ (Inertia parameter or Forchhimer number)

$$G=\frac{g\beta(T_e-T_i)a^3}{\nu^2} \quad \alpha=\frac{Qa^2}{k_fC_p}$$

$$D^{-1}=\frac{a^2}{k} \quad P_r=\frac{\mu C_p}{k_f} \quad Sc=\frac{\nu}{D_B}$$

$$\gamma=\frac{k_c^1a^2}{D_B}$$

The corresponding non-dimensional conditions are

ISSN (Online) 2456-1290

International Journal of Engineering Research in Mechanical and Civil Engineering (IJERMCE)
Vol 2, Issue 3, March 2017

$u = 0$, $\theta = 0$, C=0 at r=1 and 1+s (15)

III. FINITE ELEMENT ANALYSIS

The finite element analysis is carried out along the radial distance across the circular duct with quadratic polynomial approximation functions. The variation of velocity, temperature and concentration profiles has been discussed computationally for different parameters. The Gelarkin method has been employed in the formulation of each element to obtain the global matrices for velocity, temperature and concentration.

Choose an arbitrary element e_k and let u^k, θ^k and C^k be the values of u, θ and C in the element e_k

We define the error residuals as

$$E_p^k = \frac{d}{dr}\left(r\frac{du^k}{dr}\right) + \delta G(\theta^k) - \delta(D^{-1})ru^k - \delta^2\Delta r(u^k)^2 \quad (16)$$

$$E^k{}_\theta = \frac{1}{\Pr}\frac{d}{dr}\left(r\frac{d\theta^k}{dr}\right) - ru^k - \frac{\alpha}{P_r}r\theta \quad (17)$$

$$E^k{}_c = \frac{d}{dr}\left(r\frac{dC^k}{dr}\right) - rScu^k - \gamma C^k \quad (18)$$

where u^k, θ^k & C^k are values of u, θ& C in the arbitrary element e_k. They are displayed as linear combinations in terms of respective local nodal values.

$$u^k = u_1^k\psi_1^k + u_2^k\psi_1^k + u_3^k\psi_3^k$$
$$\theta^k = \theta_1^k\psi_1^k + \theta_2^k\psi_2^k + \theta_3^k\psi_3^k$$
$$C^k = C_1^k\psi_1^k + C_2^k\psi_2^k + C_3^k\psi_3^k$$

where ψ_1^k, ψ_2^k--------- etc are Lagrange's quadratic polynomials.

Following the Gelarkin weighted residual method and integrating by parts equations (12 – 14) we get

$$\int_{rA_1}^{rB_1} r\frac{du^k}{dr}\frac{d\psi_j^k}{dr}dr - \delta G\int_{rA_1}^{rB_1} r(\theta^k)\psi_j^k dr + \delta(M_1^2)\int_{rA_1}^{rB_1} ru^k\psi_j^k dr + \delta^2\Delta\int_{rA_1}^{rB_1} r(u^k)^2\psi_j^k dr$$
$$= Q_{2\,j}^k + Q_{1\,j}^k - P\int_{rA_1}^{rB_1} r\psi_j^k dr \quad (19)$$

$$-Q_{1\,j}^k = \left[\left(\frac{du^k}{dr}\right)(r\psi_j^k)\right]r_{A_1}$$

$$-Q_{2\,j}^k = \left[\left(\frac{du^k}{dr}\right)(r\psi_j^k)\right]r_{B_1}$$

$$\int_{rA_1}^{rB_1} r\frac{d\theta^k}{dr}\frac{d\psi_j{}^k}{dr}dr + \alpha\int_{rA_1}^{rB_1} r\theta^k dr - P_r\int_{rA_1}^{rB_1} ru^k\psi_j^k dr + R_{2\,j}^k + R_{1\,j}^k \quad (20)$$

$$-R_{1\,j}^k = \left[\left(\frac{d\theta^k}{dr}\right)(r\psi_j^k)\right]r_{A_1}$$

$$R_{2\,j}^k = \left[\left(\frac{d\theta^k}{dr}\right)(r\psi_j^k)\right]r_{B_1}$$

$$\int_{rA_1}^{rB_1} r\frac{dC^k}{dr}\frac{d\psi_j{}^k}{dr}dr - \gamma\int_{rA_1}^{rB_1} rC^k dr = Sc\int_{rA_1}^{rB_1} ru^k\psi_j^k dr + S_{2\,j}^k + S_{1\,j}^k \quad (21)$$

$$-S_{1\,j}^k = \left[\left(\frac{dC^k}{dr}\right)(r\psi_j^k)\right]r_{A_1}$$

$$S_{2\,j}^k = \left[\left(\frac{dC^k}{dr}\right)(r\psi_j^k)\right]r_{B_1}$$

Writing u^k, θ^k, C^k in terms of local nodal values in (12) - (14) we get

$$\sum_{i=1}^{3}u^k\int_{rA_1}^{rB_1} r\frac{d\psi_i^k}{dr}\frac{d\psi_j^k}{dr}dr - \delta G\sum_{i=1}^{3}(\theta_i^k)\int_{rA_1}^{rB_1} r\psi_i^k\psi_j^k dr + \frac{1}{A_1A_3}\delta(D^{-1}\sum_{i=1}^{3}\int_{rA_1}^{rB_1} r\psi_i^k\psi_j^k dr$$
$$+\delta^2\Delta\sum_{i=1}^{3}u_i^k\int_{rA_1}^{rB_1} rU_i^k\psi_i^k\psi_j^k dr = Q_{2\,j}^j + Q_{1\,j}^k - P\int_{rA_1}^{rB_1} r\psi_i^k\psi_j^k dr \quad (22)$$

$$\frac{1}{\Pr}\sum_{i=1}^{3}\theta_i^k\int_{rA_1}^{rB_1} r\frac{d\psi_i^k}{dr}\frac{d\psi_j^k}{dr}dr - \sum_{i=1}^{3}u_i^k\int_{rA_1}^{rB_1} r\psi_i^k\psi_j^k dr + \alpha\sum_{i=1}^{3}\theta_i^k\int_{rA_1}^{rB_1} r\psi_i^k\psi_j^k dr = R_{2\,j}^k + R_{1\,j}^k \quad (23)$$

$$\sum_{i=1}^{3}C_i^k\int_{rA_1}^{rB_1} r\frac{d\psi_i^k}{dr}\frac{d\psi_j^k}{dr}dr - \gamma\sum_{i=1}^{3}C_i^k\int_{rA_1}^{rB_1} r\psi_i^k\psi_j^k dr + Sc\sum_{i=1}^{3}u_i^k\int_{rA_1}^{rB_1} r\psi_i^k\psi_j^k dr = S_{2\,j}^k + S_{1\,j}^k \quad (24)$$

Choosing different ψ_j^k's corresponding to each element e_k in the equation (22 - 24) gives rise to a local stiffness matrix

ISSN (Online) 2456-1290

International Journal of Engineering Research in Mechanical and Civil Engineering (IJERMCE)
Vol 2, Issue 3, March 2017

of order 3×3 in the form

$$(f_i^k{}_j)(u_i^k)-\delta G(g_i^k{}_j)(\theta_i^k)+\delta D^{-1}(m_i^k{}_j)(u_i^k)+\delta^2\Delta(n_i^k{}_j)(u_i^k)=(Q_2^k{}_j)+(Q_1^k{}_j)+(v_j^k) \quad (25)$$

$$(e_i^k{}_j)(\theta_i^k)+\alpha(f_i^k{}_j)(\theta_i^k)-(t_i^k{}_j)(u_i^k)=R_2^k{}_j+R_1^k{}_j \quad (26)$$

$$(l_i^k{}_j-\gamma)(C_i^k)=S_2^k{}_j+S_1^k{}_j \quad (27)$$

where

$(f_i^k{}_j)$, $(g_i^k{}_j)$, $(m_i^k{}_j)$, $(n_i^k{}_j)$, $(e_i^k{}_j)$, $(l_i^k{}_j)$, $(r_i^k{}_j)$ and $(t_i^k{}_j)$ are 3×3 matrices

and $v_j^k=-P_1\int_{rA_1}^{rB_1} r\psi_i^k\psi_j^k dr$ and $(Q_2^k{}_j)$, $(Q_1^k{}_j)$, $(R_2^k{}_j)$ & $(R_1^k{}_j)$, $(S_2^k{}_j)$ & $(S_1^k{}_j)$ are 3×1 column matrices. Such stiffness matrices (25) - (27) in terms of local nodes in each element are assembled to obtain the coupled global matrices in terms of global nodal values of u , θ & C in the region.

The shape functions in the region are

$$\psi_1^1=\frac{50(-1+r-\frac{s}{5})(-1+r-\frac{s}{10})}{s^2}$$

$$\psi_2^1=\frac{100(-1+r)(-1+r-\frac{s}{5})}{s^2}$$

$$\psi_3^1=\frac{50(-1+r)(-1+r-\frac{s}{10})}{s^2}$$

$$\psi_1^2=\frac{50(-1+r-\frac{2s}{5})(-1+r-\frac{3s}{10})}{s^2}$$

$$\psi_2^2=-\frac{100(-1+r-\frac{2s}{5})(-1+r-\frac{s}{5})}{s^2}$$

$$\psi_3^2=\frac{50(-1+r-\frac{3s}{5})(-1+r-\frac{s}{5})}{s^2}$$

$$\psi_1^3=\frac{50(-1+r-\frac{3s}{5})(-1+r-\frac{s}{2})}{s^2}$$

$$\psi_2^3=-\frac{100(-1+r-\frac{3s}{5})(-1+r-\frac{2s}{5})}{s^2}$$

$$\psi_3^3=\frac{50(-1+r-\frac{s}{2})(-1+r-\frac{2s}{5})}{s^2}$$

$$\psi_1^4=\frac{50(-1+r-\frac{4s}{5})(-1+r-\frac{7s}{10})}{s^2}$$

$$\psi_2^4=-\frac{100(-1+r-\frac{4s}{5})(-1+r-\frac{3s}{5})}{s^2}$$

$$\psi_3^4=\frac{50(-1+r-\frac{7s}{10})(-1+r-\frac{3s}{5})}{s^2}$$

$$\psi_1^5=\frac{50(-1+r-s)(-1+r-\frac{9s}{10})}{s^2}$$

$$\psi_2^5=-\frac{100(-1+r-s)(-1+r-\frac{4s}{5})}{s^2}$$

$$\psi_3^5=\frac{50(-1+r-\frac{9s}{10})(-1+r-\frac{4s}{5})}{s^2}$$

The global matrix for θ is $A_3X_3=B_3$

The global matrix for C is $A_4X_4=B_4$

The global matrix for u is $A_5X_5=B_5$

where A_3, A_4, A_5 are n X n matrices B_3, B_4, B_5 are column matrices.

IV. SOLUTION OF THE PROBLEM

Solving these coupled global matrices for velocity, temperature and concentration (22) - (24) respectively and using the iteration procedure we find the unknown global nodes through which the velocity, temperature and concentration at different radial intervals at any arbitrary axial cross sections are obtained . The expressions are given as

$$\theta(r)=\psi_1^1\theta_{11}+\psi_{21}^1\theta_{12}+\psi_3^1\theta_{13} \quad 1\le r\le1+S*0.2$$

$$=\psi_1^2\theta_{13}+\psi_2^2\theta_{14}+\psi_3^2\theta_{15} \quad 1+S*0.2\le r\le1+S*0.4$$

ISSN (Online) 2456-1290

International Journal of Engineering Research in Mechanical and Civil Engineering (IJERMCE)
Vol 2, Issue 3, March 2017

$$= \psi_1^3 \theta_{15} + \psi_2^3 \theta_{16} + \psi_3^3 \theta_{17}$$

$$1 + S*0.4 \le r \le 1 + S*0.6$$

$$= \psi_1^4 \theta_{17} + \psi_2^4 \theta_{18} + \psi_3^4 \theta_{19}$$

$$1 + S*0.6 \le r \le 1 + S*0.8$$

$$= \psi_1^{15} \theta_{19} + \psi_2^5 \theta_{20} + \psi_3^5 \theta_{21}$$

$$1 + S*0.8 \le r \le 1 + S \qquad C(r) = \psi_1^1 C_{11} + \psi_{21}^1 C_{12} + \psi_3^1 C_{13}$$

$$1 \le r \le 1 + S*0.2$$

$$= \psi_1^2 C_{13} + \psi_2^2 C_{14} + \psi_3^2 C_{15}$$

$$1 + S*0.2 \le r \le 1 + S*0.4$$

$$= \psi_1^3 C_{15} + \psi_2^3 C_{16} + \psi_3^3 C_{17}$$

$$1 + S*0.4 \le r \le 1 + S*0.6$$

$$= \psi_1^4 C_{17} + \psi_2^4 C_{18} + \psi_3^4 C_{19}$$

$$1 + S*0.6 \le r \le 1 + S*0.8$$

$$= \psi_1^{15} C_{19} + \psi_2^5 C_{20} + \psi_3^5 C_{21}$$

$$1 + S*0.8 \le r \le 1 + S$$

$$u(r) = \psi_1^1 u_{11} + \psi_{21}^1 u_{12} + \psi_3^1 u_{13}$$

$$1 \le r \le 1 + S*0.2$$

$$= \psi_1^2 u_{13} + \psi_2^2 u_{14} + \psi_3^2 u_{15}$$

$$1 + S*0.2 \le r \le 1 + S*0.4$$

$$= \psi_1^3 c_{15} + \psi_2^3 c_{16} + \psi_3^3 c_{17}$$

$$1 + S*0.4 \le r \le 1 + S*0.6$$

$$= \psi_1^4 u_{17} + \psi_2^4 u_{18} + \psi_3^4 u_{19}$$

$$1 + S*0.6 \le r \le 1 + S*0.8$$

$$= \psi_1^{15} u_{19} + \psi_2^5 u_{20} + \psi_3^5 u_{21}$$

$$1 + S*0.8 \le r \le 1 + S$$

V. SHEAR STRESS,NUSSELT NUMBER AND SHERWOOD NUMBER

The shear stress (τ) is evaluated using the formula $\tau = (\frac{du}{dr})_{r=1,1+s}$

The rate of heat transfer (Nusselt number) is evaluated using the formula

$$Nu = -(\frac{d\theta}{dr})_{r=1,1+s}$$

The rate of mass transfer (Sherwood number) is evaluated using the formula $Sh = -(\frac{dC}{dr})_{r=1,1+s}$

VI. RESULTS AND DISCUSSION

The equations governing the flow, heat and mass transfer have been solved by employing Galerkin finite element analysis with quadratic approximation polynomials. The velocity, temperature and concentration profiles for different parameters are discussed graphically in below figures.

Fig.1 represents the variation of nanofluid velocity with Grashof number G. It is seen that an increase in thermal buoyancy parameter G leads to dicrease in the nano-fluid velocity field in Ti02-water nanofluid following the fact that an increase in G dicreases the thickness of the momentum boundary layer. Fig.2 exhibits the effect of inverse Darcy parameter D^{-1} on the nanofluid velocity profile. From the figure it is observed that the velocity distribution decreases with increasing the inverse Darcy parameter D^{-1}. This is due to the fact that the obstruction of the fluid motion increases with increase in the inverse Darcy parameter. Fig.3 illustrates that with the increasing values of heat source parameter α the velocity decreases. This is due to the fact that when heat is absorbed, the buoyancy forces increases which reduces the flow rate and there by gives rise to a decrease in the velocity profile. Figs.4 exhibits the influence of nanoparticle volume fraction ϕ on the nanofluid velocity. It is observed that increase in the nanoparticle volume fraction decreases the nanofluid velocity in both types of nanofluid. When the volume of the nanoparticle decreases the thermal conductivity and hence reduces the momentum boundary layer thickness. Fig.5 exhibits the variation of velocity with Forchheimer number(Δ) . It is found that increasing values of Δ in the flow region increases the velocity. This is due to the fact that the boundary layer thickness enhances with values of Δ in Tio2-water nanofluid.

Fig.6 exhibits the temperature with thermal buoyancy parameter G. From figure it can be seen that with the increasing values of G the temperature reduces in the entire flow region. This is due to the fact that the thermal buoyancy reduces the thickness of the thermal boundary layer in both types of nanofluid. Fig.7 displays the effect of inverse Darcy parameter D^{-1} on the nanofluid temperature

ISSN (Online) 2456-1290

International Journal of Engineering Research in Mechanical and Civil Engineering (IJERMCE)
Vol 2, Issue 3, March 2017

distribution. It is seen that the temperature profile decreases with increasing values of D^{-1}. This phenomenon has good agreement with the physical realities. Fig.8 illustrates the influence of the temperature with heat source parameter α. It is observed that the temperature enhances with increase in the strength of the heat generating source in the left half and increases in the right half of the annular region. In the case of heat absorbing source,it enhances in the middle region and decrases in the regions adjacent to the cylinder. This is due to the fact that the presence of the heat source produces energy in the thermal boundary layer and as a result the temperature increases in the annular region. In the case of heat absorption ($\alpha<0$) the temperature decreases with decreasing values of $\alpha<0$ owing absorption of energy in the thermal boundary layer in both types of nanofluid. Fig.9 shows that the variation of temperature with nanoparticle volume fraction ϕ. It is observed that an increase in the nanoparticle volume fraction ϕ the temperature decreases in the boundary layer. Fig. 10 shows the variation of temperature with Forchheimer number(Δ). It is observed that an increasing values in Δ increases the temperature in the thermal boundary layer.

Fig.11 represents the variation of concentration with Grashof number G. It is observed that the increasing values of thermal buoyancy parameter is decreases the concentration throughout the boundary layer. Fig.12 exhibits the effect of inverse Darcy parameter D^{-1} on the nanofluid concentration profile. It is seen that the concentration profile enhances with increasing values of darcy parameter as a result of increasing the thickness of the solutal boundary layer owing to the Darcy drag developed by the porous medium. Figure 13 represents the variation of concentration with heat source parameter α. From the figure it is observed that the concentration diminishes with increase in the strength of the heat generating source and increases with that of heat absorbing source. Fig.14 represents concentration with Schmidt number Sc. It is observed that the concentration increases with increasing values of Schmidt parameter Sc. Fig. 15 represents the variation of concentration with chemical reaction parameter γ. It is observed that in degenerating chemical reaction case the concentration increases and in the generating chemical reaction case we observe decrease in the concentration in both types of nanofluid.The effect of skin friction, Nusselt number and Sherwood number for different variations are shown in tables().

VII. CONCLUSIONS

The coupled equations governing the flow, heat and mass transfer have been solved by using Galerkin finite method with quadratic approximation functions. The velocity, temperature and concentration have been analysed for different parametric variations. The important conclusions of the analysis are

- With the increase of Grashof number G the velocity , temperature and the concentration decreases in the flow region also the skin friction, Nusselt and Sherwood number decreases with G on the cylinders.
- Decrease in the permeability of the porous medium diminishes the velocity, temperature whereas the concentration increases. The skin friction, the rate of Nusselt number reduces while the rate of Sherwood number at the boundaries enhances with D^{-1}.
- With increase in Sc the skin friction and rate of heat transfer reduces on both the cylinders but the rate of mass transfer increases on both the cylinders.
- Increase in the strength of heat generating source the velocity, temperature and the concentration decreases whereas the velocity, concentration enhances while the temperature enhances in the case of heat absorption source.The skin friction ,the Nusselt and Sherwood number decreases with increase in $\alpha>0$ and increases with $\alpha<0$ on both the cylinders.
- We find that the concentration enhances in the flow region in the degenerating chemical reaction case while in the generating chemical reaction case, it reduces in the flow region. The skin friction and Nusselt number reduces in the degenerating chemical reaction case and in the generating case, it enhances on the cylinders whereas the Sherwood number enhances in the degenerating chemical reaction case while in generating case a reversed effect is observed on the cylinders.
- Increase in the values of ϕ reduces the velocity and temperature whereas the skin friction and the Rate of heat transfer decreases while the Sherwood number enhances on the boundaries.

An increasing values of Forchheimer number Δ, increases the velocity and temperature in the annular region. The skin friction, the Nusselt and Sherwood

ISSN (Online) 2456-1290

International Journal of Engineering Research in Mechanical and Civil Engineering (IJERMCE)
Vol 2, Issue 3, March 2017

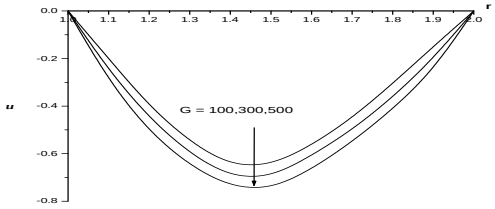

Fig. 1 : Variation of u with G
D-1=0.2, α=2, ϕ=0.1, Δ=2

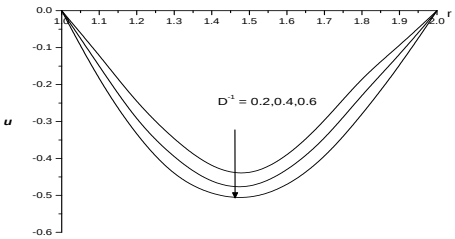

Fig. 2 : Variation of u with D^{-1}
G=2, α=2, ϕ=0.1, Δ=2

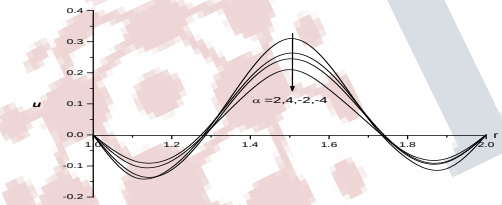

Fig. 3 : Variation of u with α
D-1=0.2, G=2, ϕ=0.1, Δ=2

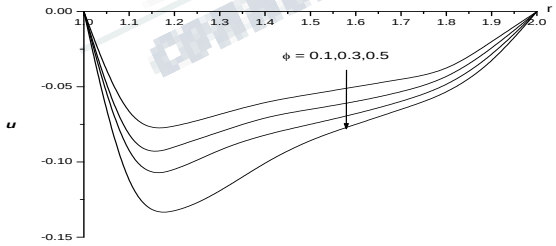

Fig. 4 : Variation of u with ϕ
D-1=0.2, α=2, G=2, Δ=2

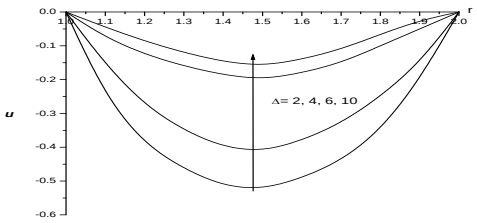

Fig. 5: Variation of u with Δ
D-1=0.2, α=2, ϕ=0.1, G=2

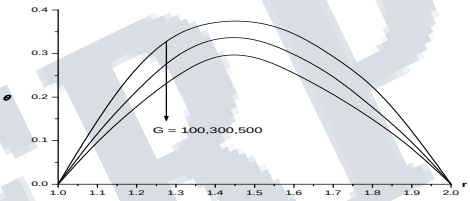

Fig. 6 : Variation of θ with G
D-1=0.2, α=2, ϕ=0.1, Δ=2

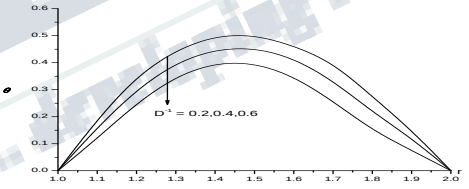

Fig.7: Variation of θ with D^{-1}
G=2, α=2, ϕ=0.1, Δ=2

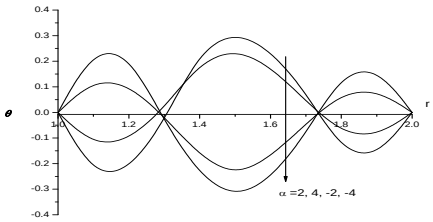

Fig.8: Variation of θ with α
D-1=0.2, G=2, ϕ=0.1, Δ=2

ISSN (Online) 2456-1290

International Journal of Engineering Research in Mechanical and Civil Engineering (IJERMCE)
Vol 2, Issue 3, March 2017

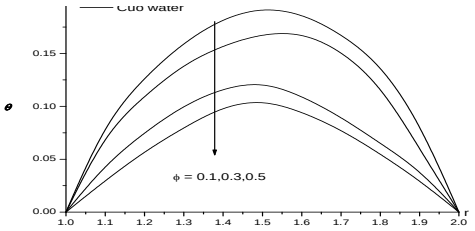

Fig. 9: Variation of θ with ϕ
D-1=0.2, α=2, G=2, Δ=2

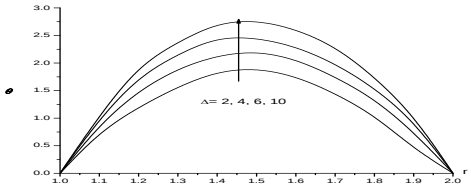

Fig. 10: Variation of θ with Δ
D-1=0.2, α=2, ϕ=0.1, G=2

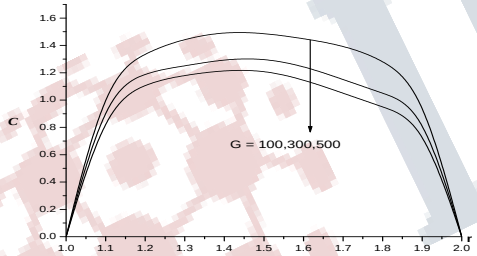

Fig. 11 : Variation of C with G
D-1=0.2, α=2, ϕ=0.1, Δ=2

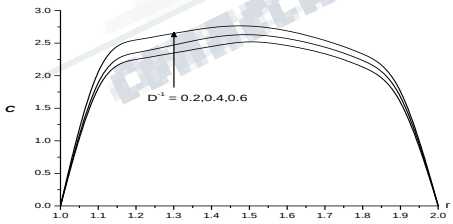

Fig. 12 : Variation of C with D-1
G=2, α=2, ϕ=0.1, Δ=2

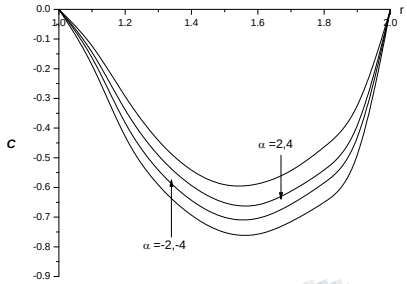

Fig. 13: Variation of C with α
D-1=0.2, G=2, ϕ=0.1, Δ=2

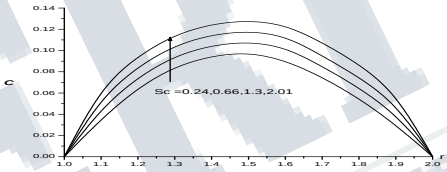

Fig. 14: Variation of C with Sc
D-1=0.2, G=2, ϕ=0.1, Δ=2,γ=0.5

The skin friction, Nusselt number and Sherwood number at inner and outer cylinders.

		(τ)(1)	(τ)(2)	Nu(1)	Nu(2)	Sh(1)	Sh(2)
G	10	-0.025754	0.01698	0.092576	-0.066176	-0.09682	0.09112
	20	-0.0229827	0.0164287	0.089571	-0.064027	-0.08524	0.08350
	30	-0.022972	0.0164209	0.089531	-0.063996	-0.08546	0.08367
D-1	0.2	-0.025754	0.01698	0.092576	-0.066176	-0.09682	0.09112
	0.4	0.00901769	0.0022048	-0.035145	-0.064027	-0.17814	0.10188
	0.6	-0.0137402	0.0098111	0.053549	-0.063996	-0.5430	0.4644
Δ	2	-0.025754	0.01698	0.092576	-0.066176	-0.09682	0.09112
	4	-0.0553739	0.0395842	0.051976	-0.045136	-0.20483	0.02007
	6	-0.120127	0.0858723	0.024463	-0.010965	-0.44432	0.04355
α	2	-0.025754	0.01698	0.092576	-0.066176	-0.09682	0.09112
	4	-0.0219927	0.0164364	0.089865	-0.064198	-0.08502	0.08336
	-2	-0.0229827	0.0174364	0.089217	-0.063772	-0.08502	0.08336
	-4	-0.0239927	0.0184364	0.089022	-0.063814	-0.08502	0.08336
ϕ	0.1	-0.025754	0.01698	0.092576	-0.066176	-0.09682	0.09112
	0.3	-0.0171517	-0.0124562	0.066844	0.485454	-0.07652	0.042477
	0.5	0.007212354	-0.0041264	-0.028108	0.016082	-0.05613	0.038515
Sc	0.3	-0.0250082	0.0164486	0.896694	-0.064105	-0.01564	0.01534
	0.6	-0.025754	0.0164437	0.090501	-0.064099	-0.04325	0.04238
	1.3	-0.025754	0.01698	0.092576	-0.064085	-0.09682	0.09112
γ	0.5	-0.025754	0.01698	0.092576	-0.066176	-0.09682	0.09112
	1.5	-0.0229919	-0.0229919	0.089606	-0.064055	-0.011717	0.010694
	-0.5	-0.0229933	0.0164369	0.089611	-0.064059	-0.05958	0.06459
	-1.5	-0.0229938	0.0164373	0.089656	-0.064065	-0.03904	0.04926

ISSN (Online) 2456-1290

International Journal of Engineering Research in Mechanical and Civil Engineering (IJERMCE)
Vol 2, Issue 3, March 2017

REFERENCES

[1] Maxwell, J.C: Electricity and magnetism, Clarendon Press, Oxford, UK (1873).
[2] Choi, S.U.S: Enhancing thermal conductivity of fluid with nanoparticles, developments and applications of non-Newtonian flow, ASME FED 231, pp.99-105(1995).
[3] Wen, D and Ding, Y: Formulation of nanofluids for natural convective heat transfer applications, Int J Heat Fluid Flow, V. 26(6), pp.855-864(2005).
[4] Mokhtari Moghari, R., Akbarinia, A., Shariat, M., Talebi, F., Laur, R: Two phase mixed convection Al_2O_3-water nanofluid flow in an annulus, Int J Multiph Flow, V.37(6), pp.585-595(2011).
[5] Abu-Nada, E., Masoud, Z., Hijazi, A: Natural convection heat transfer enhancement in horizontal concentric annuli using nanofluids, Int Commun Heat Mass Transf, V.35, 657-665(2008).
[6] Srinivas , S., Vijaya Lakshmi. A: Hydromagnetic flow of a nano fluid in a porous channel with expanding or contracting walls, J. of porous media, 17(11), (2014).
[7] Nagasasikala, M and Phrabhakar Rao G: Heat and mass transfer of a MHD flow of a nanofluid through a porous medium in an annular, circular region with outer cylinder maintained at constant heat flux, Presented in NCIT Conference, SSBN Degree College, Ananatapuramu(2016).
[8] Sudarsana Reddy, P., Chamka, A.J: Soret and dufour effects on MHD convetive flow of Al2O3-water and TiO2- water nanofluids past a stretching sheet in porous media with heat generation/absorption, J. Advanced Powder Technology, V. 27, pp.1207-1218(2016).
[9] Srinivas, G., Srikanth Gorti, V.P.N., Suresh Babu, B and Sreenatha Reddy, S: Particle spacing and chemical reaction effects on convective heat transfer through a nanofluid in cylindrical annulus, Procedia Engineering, 127, pp.263-270(2015).
[10] Sheikhzadeh,G.A, Arbaban,M and Mehrabian,M.A: Laminar natural convection of Cu-Water nanofluids in concentric annuli with radial fins attached to the inner cylinder.,Heat Mass transfer.,V.49,pp.391-403(2013).